The Plant Cell, Vol. 24: 1549–1559, April 2012, www.plantcell.org

De Novo Pyrimidine Nucleotide Synthesis Mainly Occurs outside of Plastids, but a Previously Undiscovered Nucleobase Importer Provides Substrates for the Essential Salvage Pathway in *Arabidopsis* [W]

Sandra Witz,[1] Benjamin Jung,[1] Sarah Fürst, and Torsten Möhlmann[2]

Abteilung Pflanzenphysiologie, Fachbereich Biologie, Technische Universität Kaiserslautern, D-67663 Kaiserslautern, Germany

Nucleotide de novo synthesis is highly conserved among organisms and represents an essential biochemical pathway. In plants, the two initial enzymatic reactions of de novo pyrimidine synthesis occur in the plastids. By use of green fluorescent protein fusions, clear support is provided for a localization of the remaining reactions in the cytosol and mitochondria. This implies that carbamoyl aspartate, an intermediate of this pathway, must be exported and precursors of pyrimidine salvage (i.e., nucleobases or nucleosides) are imported into plastids. A corresponding uracil transport activity could be measured in intact plastids isolated from cauliflower (*Brassica oleracea*) buds. PLUTO (for plastidic nucleobase transporter) was identified as a member of the Nucleobase:Cation-Symporter1 protein family from *Arabidopsis thaliana*, capable of transporting purine and pyrimidine nucleobases. A PLUTO green fluorescent protein fusion was shown to reside in the plastid envelope after expression in *Arabidopsis* protoplasts. Heterologous expression of PLUTO in an *Escherichia coli* mutant lacking the bacterial uracil permease uraA allowed a detailed biochemical characterization. PLUTO transports uracil, adenine, and guanine with apparent affinities of 16.4, 0.4, and 6.3 μM, respectively. Transport was markedly inhibited by low concentrations of a proton uncoupler, indicating that PLUTO functions as a proton-substrate symporter. Thus, a protein for the absolutely required import of pyrimidine nucleobases into plastids was identified.

INTRODUCTION

Nucleotides are building blocks of RNA. Both nucleotides and RNA are among the first biomolecules to arise in the evolution of life long before DNA and proteins came into play (Joyce, 2002). Since that time, nucleotide and nucleic acid metabolism have constituted a central part of the metabolism of every living organism. Because of the early appearance in evolution and the essential importance for life, nucleotide de novo synthesis is highly similar in almost all living organisms (Lehninger et al., 1994; Kafer et al., 2004). In *Arabidopsis thaliana*, all enzymatic steps are encoded by single genes, and lack of function of any of the genes is lethal (Schröder et al., 2005). Carbamoylphosphate synthetase, which catalyzes the first step in pyrimidine de novo synthesis, is different as it is composed of two subunits, and two transcripts encoding the small subunit were identified in *Medicago truncatula* (Brady et al., 2010). This allows a flexible regulation of pyrimidine de novo synthesis independent from Arg synthesis, a second pathway for which carbamoylphosphate serves as precursor (Brady et al., 2010).

The second enzyme in pyrimidine de novo synthesis, aspartate carbamoyltransferase (ATCase), is described as a plastid-localized enzyme (Chen and Slocum, 2008). N-(phosphonacetyl)-L-aspartate is a potent inhibitor of ATCase, and seeds treated with this agent grow only until day 5 and then arrest. This arrest can be reversed by adding the nucleobase uracil (Chen and Slocum, 2008). In general, it is assumed that pyrimidine de novo synthesis is exclusively located in plastids with the exception of the reaction catalyzed by dihydroorotate dehydrogenase (DHODH) (Slocum, 2005). However, direct experimental evidence for this assumption is lacking.

The role of plastids in pyrimidine catabolism and salvage has been in the focus of recent work and can be regarded as well established. Salvage can take place at the level of nucleosides or nucleobases. Plastid-localized uridine kinase isoforms from *Arabidopsis* have been identified, and double knockouts were shown to exhibit a dwarf phenotype, indicating an important function of uridine salvage in plastids (Chen and Thelen, 2011). However, it is unclear whether or how uridine is imported into plastids. Pyrimidine and purine-nucleoside cleavage is mainly facilitated by nucleoside hydrolase1 (NSH1), a cytosolic enzyme (Jung et al., 2009, 2011, Riegler et al., 2011). The resulting nucleobases can then undergo either salvage by phosphoribosyl-pyrophosphate–dependent phosphoribosyl-transferases or catabolism. The main salvage activity of uracil was reported to be present in plastids. Lack of the corresponding enzyme UPP in T-DNA insertion mutants leads to an albino phenotype (Mainguet et al., 2009). Interestingly, both uridine and uracil salvage are mainly located to plastids, and lack of either activity has severe consequences for overall growth performance of *Arabidopsis* plants.

Whereas catabolism of purine bases takes place without participation of plastidic enzymes (reviewed in Werner and Witte,

[1] These authors contributed equally to this work.
[2] Address correspondence to moehlmann@biologie.uni-kl.de.
The author responsible for distribution of materials integral to the findings presented in this article in accordance with the policy described in the Instructions for Authors (www.plantcell.org) is: Torsten Möhlmann (moehlmann@biologie.uni-kl.de).
[W] Online version contains Web-only data.
www.plantcell.org/cgi/doi/10.1105/tpc.112.096743

2011), the first step in pyrimidine base (uracil and thymine) conversion by PYD1 is clearly located in plastids (Zrenner et al., 2009; Cornelius et al., 2011). Knocking out PYD1 affects germination performance of seeds, as does downregulation of NSH1 (Jung et al., 2009; Cornelius et al., 2011). Keeping the balance between nitrogen liberation by pyrimidine catabolism versus pyrimidine salvage is important especially during seed germination. For plants, this process is meaningful as nitrogen limitation often constrains growth. When nucleotides are degraded to the level of nucleosides or nucleobases, these intermediates can be exchanged between cells by corresponding transport proteins, allowing for a high flexibility of nucleotide metabolism at the level of tissues or whole organisms (Möhlmann et al., 2010). Nucleosides or nucleobases can be recycled to nucleotides by the salvage pathway, which is less energy consuming compared with nucleotide de novo synthesis. Whereas nucleotides can be exchanged between the cytosol, organelles, peroxisomes, and the endoplasmic reticulum, no significant transport is possible across the plasma membrane (Geigenberger et al., 2010; Möhlmann et al., 2010). Therefore, nucleosides and nucleobases can be regarded as transport form of purine and pyrimidine metabolites. In this work, we aim to deepen our understanding related to transport of nucleobases, especially uracil, across the plastid envelope and the significance of this process in the context of the subcellular distribution of pyrimidine de novo synthesis.

RESULTS

Uracil Uptake into Isolated Plastids

The initial aim of this work was to identify a uracil import system in plastids. From the recently published work, it became obvious that such an import system must exist because subsequent enzymatic steps in nucleoside salvage and catabolism are distributed between plastid and cytosol (for details, see Introduction). To obtain experimental evidence for the capacity of plastids to import uracil, cauliflower (*Brassica oleracea*) buds were chosen as source tissue for plastid isolation. Heterotrophic plastids from cauliflower can be isolated with high purity and intactness and were shown to be capable of transporting various metabolites, such as triose and hexose phosphates and ATP (Neuhaus et al., 1993). Uptake of [^{14}C]-uracil into isolated plastids was determined by the silicone oil technique. Import of uracil (10 μM) was linear with time for at least 10 min and accounted for 100 $\pm$ 13 nmol g^{-1} protein h^{-1}. The concentration-dependent uptake of uracil into plastids followed Michaelis-Menten kinetics and revealed an apparent affinity of 12.6 μM (Figure 1). The activity of the salvage pathway enzyme uracil phosphoribosyltransferase (UPRT) was also radiometrically assayed in isolated cauliflower plastids and accounted for 5.6 $\pm$ 0.5 μmol g^{-1} protein h^{-1}.

Biochemical Characterization of PLUTO, a Nucleobase Transport Protein

Yeast cells import uracil via the nucleobase permease FUR4 to support pyrimidine nucleotide salvage (Chevallier and Lacroute, 1982; Jund et al., 1988; Mitterbauer et al., 2002). FUR4 belongs to the Nucleobase:Cation Symporter1 (NCS1) family of transport proteins, also known as purine-related transporters (Saier et al., 2009; www.tcdb.org). The closest *Arabidopsis* homolog to this protein is encoded by At5g03555. The deduced amino acid sequence exhibits 23% identity and 43% similarity to FUR4 (Figure 2). The N terminus of the At5g03555 translation product contains a predicted target sequence for chloroplasts (ChloroP_v1.1; Emanuelsson et al., 1999). Therefore, this protein represented a good candidate for a plastidic uracil importer and was named PLUTO (for plastidic nucleobase transporter). PLUTO encodes a protein of 599 amino acids in length with a calculated molecular mass of 65.4 kD. Furthermore, PLUTO is a highly hydrophobic membrane protein with 12 predicted transmembrane α-helical spanners, which is typical for NCS1 family members (Schwacke et al., 2003; Saier et al., 2009). The first structure of a NCS1 family member was solved from *Microbacterium liquefaciens* (Weyand et al., 2008); in that work, 34 highly conserved amino acid residues were identified in NCS1 members from bacteria and fungi. Thirty of these residues are also conserved in PLUTO (Figure 2, marked by a black background).

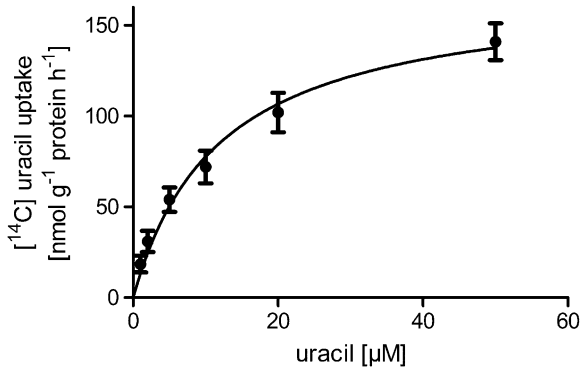

Figure 1. Uracil Uptake into Isolated Cauliflower Bud Amyloplasts.

Uptake of [^{14}C]-uracil into isolated cauliflower bud amyloplasts was determined by silicone oil centrifugation after incubation for 2 min at room temperature. An apparent K_m value of 12.6 μM was calculated. Data represent the mean of at least six independent experiments ($\pm$SE).

PLUTO expression was induced in *Escherichia coli* mutants lacking the bacterial endogenous uracil permease uraA, obtained from the National Institute of Genetics, Shizuoka, Japan (www.nig.ac.jp/). After induction of *PLUTO* expression, *E. coli* cells showed uptake of [^{14}C]-uracil in a time-dependent manner. Uracil uptake was linear for at least 5 min and then accounted for 3.75 μmol mg^{-1} protein, whereas noninduced cells imported only 0.52 μmol mg^{-1} protein (Figure 3A). The apparent affinity of PLUTO for uracil was 16.4 μM (Figure 3B). A detailed analysis of the substrate specificity was performed by direct uptake studies of the nucleobases adenine and guanine. Time-dependent uptake studies with [^{14}C]-adenine showed clearly increasing uptake upon induction, whereas uptake into noninduced *E. coli* cells remained low (Figure 4A). After 5 min, induced cells imported 4.8 μmol adenine g^{-1} protein and controls only 1.5 μmol adenine g^{-1} protein (Figure 4A): Uptake was linear for $\sim$5 min. Similar results

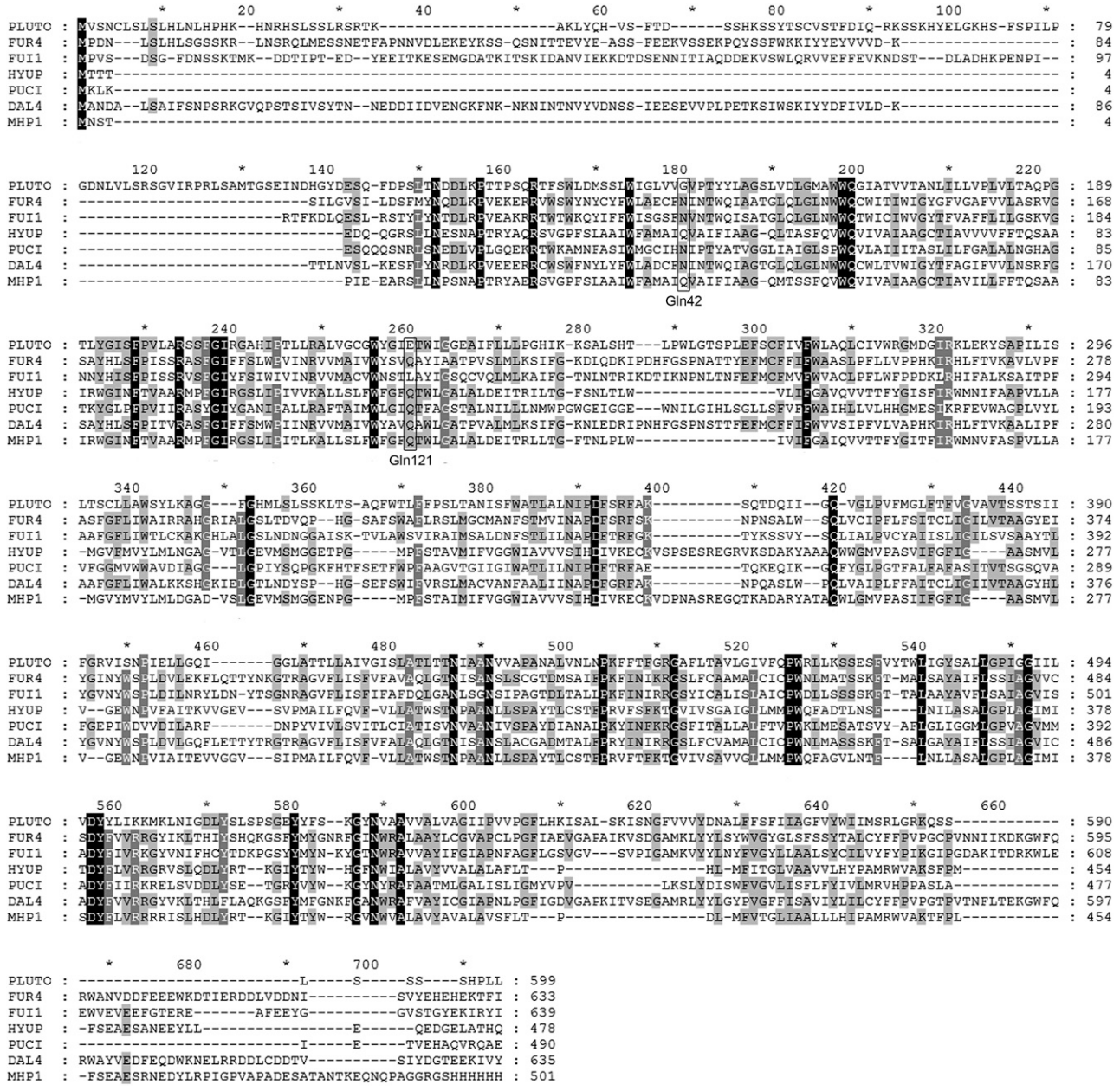

Figure 2. Alignment of NCS1-Type Protein Sequences from Different Organisms.

NCS1 proteins from *Arabidopsis* (PLUTO), *S. cerevisiae* (FUR4, FUI1, and DAL4), *Arthrobacter aurescens* (HYUP), *Bacillus subtilis* (PUCI), and *M. liquefaciens* (MHP1) were aligned using the ClustalW program of the EMBL European Bioinformatics Institute (www.ebi.ac.uk). Conserved amino acid residues are shown with a black background.

were obtained for [^{14}C]-guanine uptake. After 5 min, induced cells imported 3.9 μmol guanine g^{-1} protein and controls only 0.5 μmol guanine g^{-1} protein (Figure 4A). The apparent affinities for adenine and guanine uptake calculated by subtracting the uptake rates of noninduced cells in substrate-dependent import studies were as follows: 0.38 μM for adenine (Figure 4B) and 6.29 μM for guanine (Figure 4C).

To check whether nucleosides are also substrates of PLUTO, these were tested in corresponding uptake studies. However, when radiolabeled uridine was supplied to *E. coli* cells and cellular extracts were subsequently run on thin layer chromatography, a fast cleavage to the corresponding nucleobases was observed (see Supplemental Figure 1 online). Cleavage is assumed to occur in the periplasmic space of the bacterial cells by corresponding enzyme activities as shown for adenosine (Watanabe et al., 2011). Therefore, the question whether nucleosides are also substrates of PLUTO cannot be addressed with this experimental system.

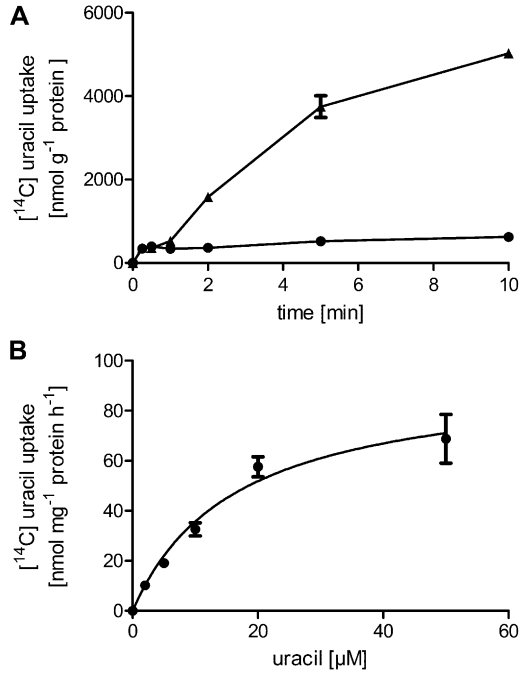

Figure 3. Time Course and Concentration Dependence of Uracil Uptake by PLUTO Heterologously Expressed in *E. coli*.

(A) Time course of [^{14}C]-uracil uptake at 20 μM substrate concentration. Circles, *E. coli* cells grown in the absence of inducer (IPTG); triangles, cells induced by IPTG.

(B) Concentration dependence of uracil uptake. Uptake was measured for 2 min. Data represent the mean of at least six independent experiments (±SE).

Some of the characterized NCS1 proteins function as nucleobase-sodium symporters (Saier et al., 2009). To test whether this also holds true for PLUTO, uracil uptake was measured in the presence of 25 or 50 mM sodium in the uptake medium. However, no effect of sodium upon uracil transport was observed compared with controls without addition of cations or 25 mM LiCl (Figure 5A). Instead, the protonophore *m*-chlorophenylhydrazone (CCCP) inhibited uracil transport almost completely at relatively low concentrations of 25 μM (Figure 5B). The addition of 5 μM CCCP resulted in 75% lower uptake activity, and 25 μM CCCP reduced uracil uptake to 7%, compared with untreated samples (Figure 5B). Most likely, PLUTO functions as a nucleobase-proton symporter.

A PLUTO-GFP Fusion Protein Is Targeted to the Plastid Envelope

To check for the subcellular localization of PLUTO, green fluorescent protein (GFP) was translationally fused to the C-terminal end of PLUTO. Transient expression in *Arabidopsis* protoplasts revealed a clear plastidic localization of PLUTO-GFP. In single confocal slices, the red autofluorescence of chlorophyll is surrounded by GFP fluorescence, indicating a labeling of the plastid envelope (Figure 6). A GFP fusion of the plastidic ATP/ADP transporter NTT1 (Neuhaus et al., 1997) showed a similar distribution of GFP fluorescence (Figure 6). By contrast, an N-terminal truncated PLUTO-GFP construct no longer colocalized with plastids but was found in internal structures resembling a network [Figure 6, PLUTO (-)]. A similar truncated *PLUTO* construct without GFP was tested for uracil transport capacity. However, no transport activity could be detected. Particle bombardment of onion epidermal peels with PLUTO-GFP showed results in line with those observed in *Arabidopsis* protoplasts: Only plastids showed GFP fluorescence (see Supplemental Figure 2 online).

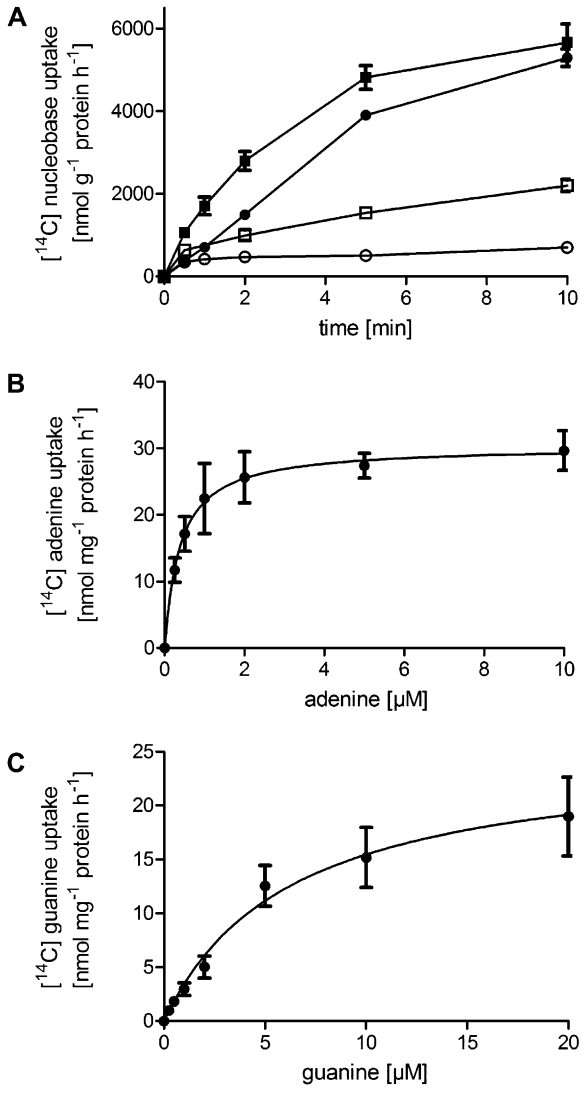

Figure 4. Time Course and Concentration Dependence of Adenine and Guanine Uptake by PLUTO Heterologously Expressed in *E. coli*.

(A) Time course of [^{14}C]-adenine (squares) and [^{14}C]-guanine (circles) uptake at 20 μM substrate concentration. Open symbols, *E. coli* cells grown in the absence of inducer (IPTG); closed symbols, cells induced by IPTG.

(B) and **(C)** Concentration dependence of adenine and guanine uptake. Uptake was measured for 2 min. Data represent the mean of at least six independent experiments (±SE).

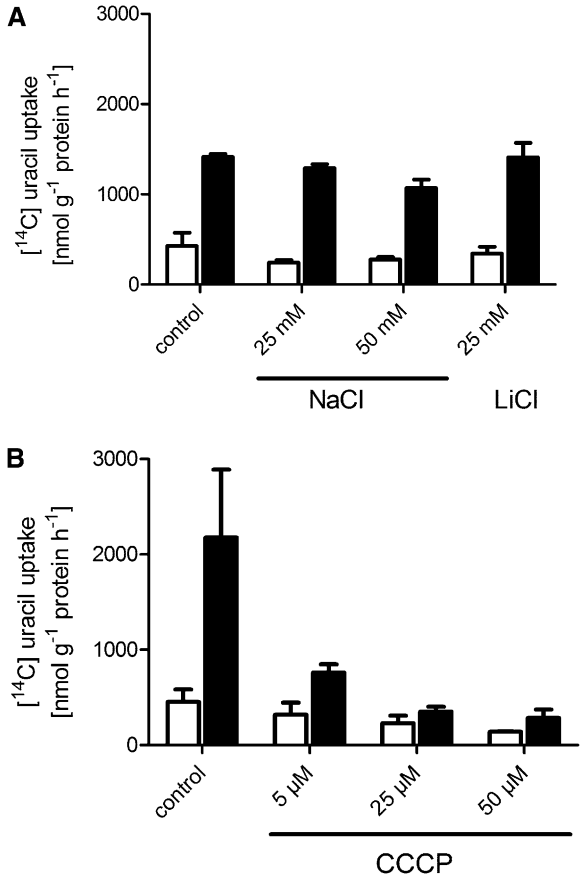

Figure 5. Effect of NaCl and the Protonophore CCCP on Uracil Uptake by *PLUTO* Heterologously Expressed in *E. coli*.

(A) Effect of NaCl and LiCl (control) on uracil uptake by *PLUTO* heterologously expressed in *E. coli*.
(B) Effect of the protonophore CCCP on uracil uptake by *PLUTO* heterologously expressed in *E. coli*.
White bars, *E. coli* cells grown in the absence of inducer (IPTG); black bars, cells induced by IPTG. Data represent the mean of at least three independent experiments (±SE).

PLUTO Function in Nucleotide Metabolism

Monitoring *PLUTO* expression by quantitative RT-PCR on cDNA from different *Arabidopsis* tissues revealed a medium transcript level in most tissues with up to 2 times higher levels in stems and seeds compared with the control gene *EF1α* (Figure 7A). On a developmental scale, higher *PLUTO* expression was observed in 2- to 10-d-old seedlings, compared with 4-week-old plants (Figure 7B). These results are in good agreement with microarray data (Zimmermann et al., 2004). Interestingly a threefold upregulation of *PLUTO* expression was observed in *PYD1* knockout mutants, defective in uracil catabolism (Figure 7B).

To address the question about a possible function of PLUTO within nucleotide metabolism, a closer look at the corresponding processes in plastids was necessary. In the case of pyrimidine de novo synthesis, it is not clear which enzymatic steps are located in plastids. To clarify this situation, the enzymes facilitating the second (ATCase, At3g20330), third (dihydroorotase [DHOase], At4g22930), fourth (DHODH, At5g23300), and fifth (orotate phosphoribosyltransferase/orotidine-5′-phosphate decarboxylase [UMPSase], At3g54470) enzymatic steps in pyrimidine de novo synthesis were synthesized as GFP fusion proteins in *Arabidopsis* protoplasts. DHOase-GFP and UMPSase-GFP fusion proteins clearly located to the cytosol, whereas DHODH-GFP was associated with mitochondria (Figure 8). Based on these results, a model describing the subcellular organization of pyrimidine metabolism in *Arabidopsis* was developed (Figure 9).

DISCUSSION

Uracil Import into Plastids Is Required for Catabolism and Salvage

Uracil import into plastids is strictly required based on the finding that catabolism of this nucleobase as well as salvage occur in this subcellular compartment, whereas the main enzyme releasing uracil, NSH1, is located in the cytosol. The corresponding enzymes have recently been characterized at the molecular level (Jung et al., 2009, 2011; Mainguet et al., 2009; Zrenner et al., 2009; Cornelius et al., 2011). Uracil catabolism in plastids, initiated by PYD1, is especially important for germination as shown for *PYD1* knockout mutants (Cornelius et al., 2011). Even more important is the capacity to salvage plastidic uracil. The main activity for UPRT encoded by *UPP* was found in plastids.

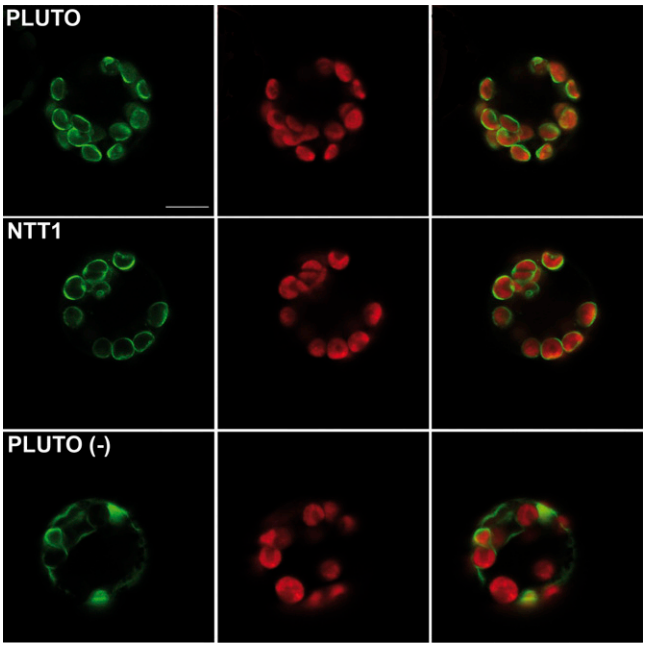

Figure 6. Localization of PLUTO-GFP Fusion Proteins Transiently Expressed in *Arabidopsis* Protoplasts.

PLUTO, NTT (plastidic nucleotide transporter, as control), and PLUTO(-) (N-terminal truncated PLUTO) GFP fusion proteins were expressed in *Arabidopsis* protoplasts. Images from left to right show GFP fluorescence, chlorophyll autofluorescence, and merge of GFP and chlorophyll fluorescence. Bar in the top left image = 10 μm; all images are the same magnification.

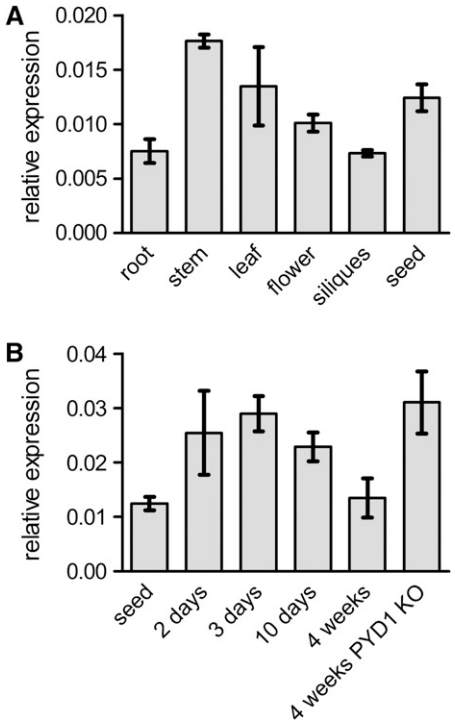

Figure 7. Relative Transcript Level of *PLUTO* Revealed by Quantitative RT-PCR.

(A) Tissue-specific expression.
(B) Expression in whole aboveground plant tissues at different stages and in a *PYD1*-knockout (KO) mutant.
Data represent the mean of at least three independent experiments (±SE).

Corresponding knockout mutants exhibited a dwarf, low chlorophyll–containing phenotype (Mainguet et al., 2009).

In this work, direct uptake of radiolabeled uracil was determined on heterotrophic plastids isolated from cauliflower buds. These plastids can be isolated with high purity and intactness (Journet and Douce, 1985) and used for uptake experiments (Neuhaus, et al., 1993; Möhlmann et al., 1994). Uptake of uracil followed Michaelis-Menten kinetics, and the apparent affinity was calculated to be 12.6 μM. V_{max} of uracil uptake was determined as 100 nmol g^{-1} protein h^{-1}, whereas the activity of the salvage pathway enzyme UPRT accounted for 5.6 μmol g^{-1} protein h^{-1} in the same plastid preparation. This means that salvage of uracil is more than sufficient to convert all imported uracil to UMP, under the given experimental conditions.

So Far, PLUTO Represents the Only Transport System for Pyrimidines across the Plastid Envelope

Until now, it was unclear how pyrimidines cross the plastid envelope. Not only is a corresponding transport system required for the purpose of pyrimidine catabolism and salvage, but also for export of end products or intermediates of pyrimidine de novo synthesis corresponding transport systems, which are lacking. As will be discussed later, it was not clear for a long time which part of pyrimidine de novo synthesis is located in plastids. By contrast, purine de novo synthesis is completely located in plastids, and a corresponding transporter was identified for export of the newly synthesized purine nucleotides with Bt1 (Kirchberger et al., 2008). However, the assumption that pyrimidine de novo

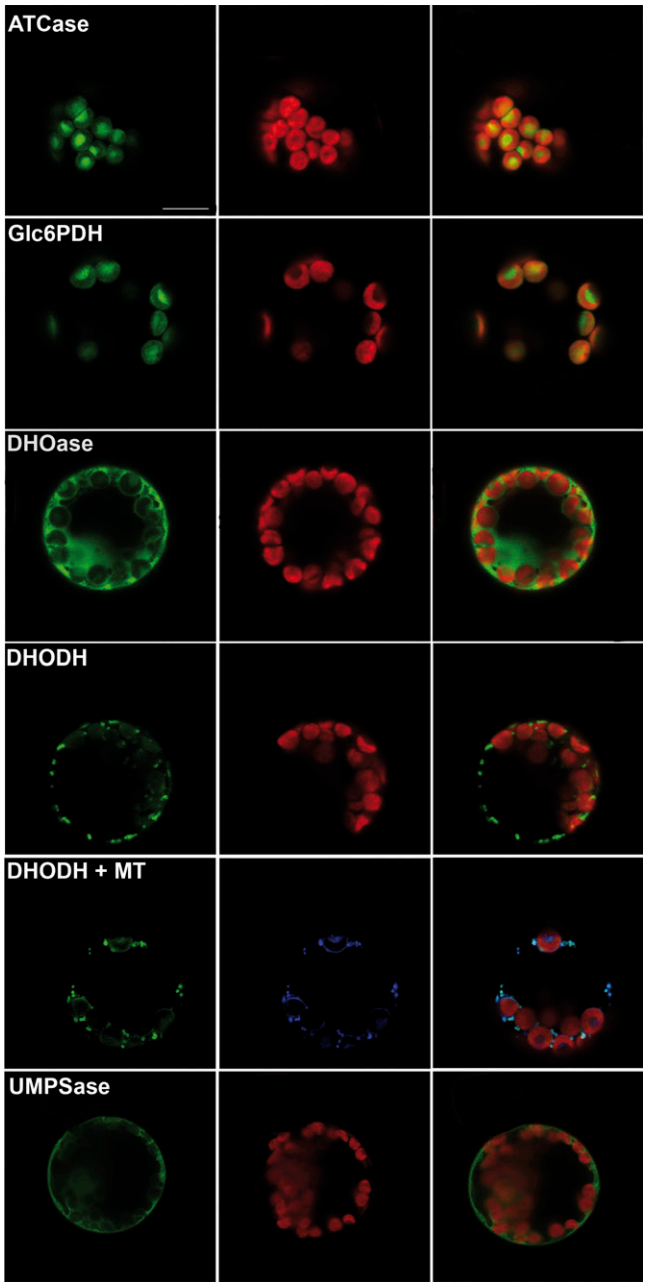

Figure 8. Localization of Enzymes of Pyrimidine de Novo Synthesis after Expression as GFP Fusion Proteins in *Arabidopsis* Protoplasts.

Images from left to right show GFP fluorescence, chlorophyll autofluorescence, and merge of GFP and chlorophyll fluorescence. DHODH+MT, colocalization of DHODH-GFP (green) and mitotracker (blue). Right image shows overlay of GFP, mitotracker, and chlorophyll autofluorescence. Bar in the top left image = 10 μm; all images are the same magnification.

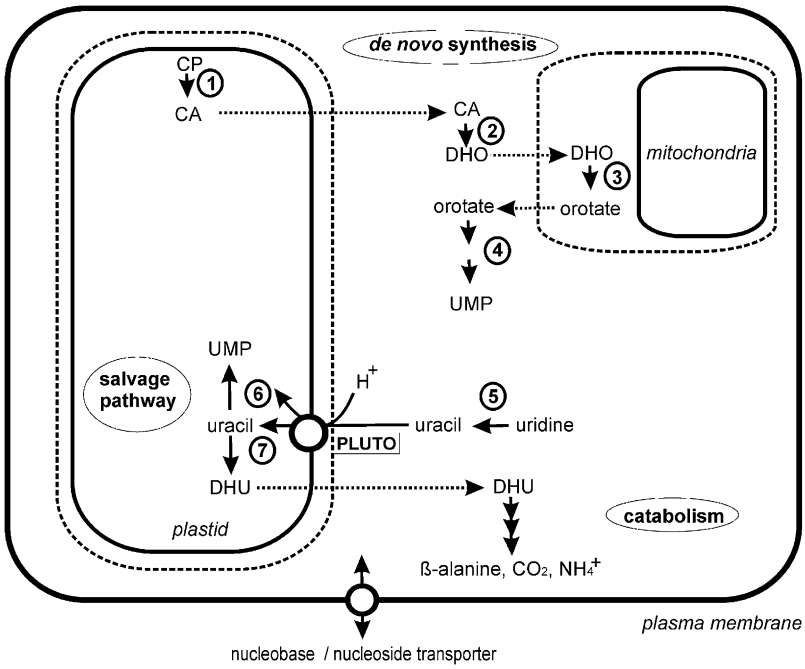

Figure 9. Schematic Overview of Selected Aspects of Pyrimidine Metabolism and Its Subcellular Localization.

De novo pyrimidine synthesis (1 to 4) is distributed in different subcellular compartments and finally UMP is formed in the cytosol. Nucleosides, here shown for uridine, appear as breakdown products from nucleotides and are cleaved by a nucleoside hydrolase (5). The product (in the case of uridine, this is uracil) then has to enter the plastid to undergo salvage (6) or the initial step in nucleobase catabolism catalyzed by PYD1 (7). Import of uracil by PLUTO is the only known mechanism to supply plastids with precursors for pyrimidine nucleotide formation. CA, carbamoyl aspartate; CP, carbamoylphosphate; DHO, dihydroorotate; DHU, dihydrouracil. PLUTO mediates uracil import into plastids. 1, ATCase; 2, DHOase; 3, DHODH; 4, UMPSase; 5, NSH1; 6, UPP, UPRT; 7, PYD1, dihydrouracil dehydrogenase.

synthesis functions similar to purine de novo synthesis with respect to the subcellular localization of enzymes and transport proteins involved is incorrect, based on our results.

Transport systems for nucleobases exist in *Arabidopsis* in a high number and are organized in different protein families (reviewed in Möhlmann et al., 2010). However, among these proteins, there is no candidate with predicted plastidic localization. *Arabidopsis* locus At5g03555 encodes a protein with significant amino acid similarity to the FUR4 uracil transporter of *Saccharomyces cerevisiae*, was predicted to be plastidic (Schwacke et al., 2003), and had not been analyzed before. After expression in an *E. coli* mutant lacking the bacterial endogenous uracil permease uraA, high-affinity uracil uptake could be determined (K_m = 16.4 μM; Figure 3B). FUR4 and PLUTO (encoded by At5g03555) belong to the NCS1 protein family (Saier et al., 2009). Members of this family function either as substrate-proton symporters or substrate-sodium symporters. In the case of PLUTO, the marked inhibitory effect of low concentrations of the uncoupler CCCP on uracil uptake indicates a substrate-proton symport mechanism. Interestingly, a plastidic pyruvate transporter was described recently for which sodium gradients were identified as the driving force for transport (Furumoto et al., 2011). However, the addition of sodium to the transport medium did not affect uracil transport by PLUTO. Thus, we conclude that PLUTO acts as a substrate-proton symporter independent from transmembrane sodium gradients (Figure 9).

The subcellular localization of PLUTO in plastid envelopes was shown by corresponding GFP fusion proteins. GFP fluorescence originating from these constructs clearly surrounded the red autofluorescence stemming from the chlorophyll within plastids. Control protoplasts expressing NTT1, the plastidic ATP/ADP carrier, as a GFP fusion look very similar. PLUTO contains an N-terminal extension relative to MHP1, and a second ATG codon was identified in frame near the end of the region coding for this extension. Therefore, GFP and expression constructs were prepared starting at one or the other putative start codon. However, the short GFP construct [Pluto(-)] showed no plastidic targeting (Figure 8), indicating that the N-terminal region contains information for targeting to plastids. Comparison to MHP1 reveals that no amino acids participating in substrate binding or transmembrane domains are present in the N-terminal extension. However, after expression of the truncated protein in *E. coli*, no uracil transport was detected, indicating that part of this N-terminal region is important for the transport function. Another explanation is to assume that the truncated PLUTO is no longer inserted into the bacterial plasma membrane.

PLUTO Is a Member of the NCS1 Protein Family

PLUTO shares 23% sequence identity to FUR4 from yeast. Both proteins belong to the NCS1 family. The structure of one family member, MHP1 from *M. liquefaciens*, was resolved at high

resolution, and amino acids involved in substrate binding were identified (Weyand et al., 2008). MHP1 represents a benzyl hydantoin transporter with 12 transmembrane helices. The structures of the outward-facing open and the substrate-bound occluded conformations were solved. Transmembrane helices 1, 3, 6, 8, and 10 form the substrate binding cavity which closes after binding (Weyand et al., 2008). Four out of six of the amino acid residues forming the substrate pocket are conserved between MHP1 and PLUTO. Gln-42 of MHP1 is thought to be involved in the substrate specificity as it can form a hydrogen bond with the nitrogen atom of the pyrimidine rings. In the protein sequences of the uracil and uridine transport proteins FUR4 and FUI1 and also in the proteins PUCI and DAL4, representing allantoin transport proteins, an Asn residue is present. PLUTO differs as a Gly residue is present at this position, allowing for high flexibility in the protein (Figure 2). This might be one reason that PLUTO can transport purine and pyrimidine substrates. A second amino acid position important in this respect is Gln-121. This residue is conserved in all compared proteins, except for FUI1 (Figure 2). However, PLUTO carries a negatively charged Glu at the corresponding position.

Plastid Pyrimidine Metabolism Depends on Salvage

It is obvious that plastids need to import uracil when pyrimidines have to be catabolized. This is because uracil appears as breakdown product from cytosolic NSH1 and is substrate for the first enzyme in pyrimidine base catabolism, PYD1, which is located in the plastid stroma (Jung et al., 2009; Zrenner et al., 2009; Cornelius et al., 2011). Furthermore, uracil breakdown was shown to be important under conditions where recycling of nitrogen from pyrimidine bases to general nitrogen is especially important. One example of such a condition is the early phase of seed germination (Cornelius et al., 2011). The high expression of *PLUTO* early in germination supports a participation in pyrimidine metabolism, as expression of *NSH1* and *PYD1* is also high during this developmental period. Furthermore, upregulation of *PLUTO* in *PYD1* knockout mutants was observed. As *PYD1* knockout mutants are no longer able to mobilize ammonia from pyrimidines, this might be perceived by a so far unknown mechanism and lead to increased *PLUTO* transcript levels to allow for increased uracil import into plastids.

The initial reactions in pyrimidine de novo synthesis catalyzed by carbamoylphosphate synthetase and ATCase take place in plastids (Shibata et al., 1986; Chen and Slocum, 2008). The results from localization studies with GFP fusion proteins presented here clearly indicate that all further steps in pyrimidine de novo synthesis are not located in the plastid stroma. DHOase and UMPSase GFP fusion proteins clearly locate outside the plastid stroma, apparently in the cytosol (Figure 8). Both proteins are not or are only weakly annotated as organellar by corresponding prediction software (Schwacke et al., 2003), supporting these results. DHODH locates to mitochondria based on GFP fusion protein analysis (Figure 8) in good agreement with previously reported data (Ullrich et al., 2002; Zrenner et al., 2006). Based on these findings, we propose the following hypothesis: Pyrimidine de novo synthesis in *Arabidopsis* is located in the plastid, mitochondrion, and cytosol. The last three steps catalyzed by DHOase, DHODH, and UMPSase are located outside the plastid stroma; thus, pyrimidine nucleotides are not synthesized de novo in this organelle but have to be imported in form of nucleosides or nucleobases and require salvage pathway activity. The first and possibly the only protein capable to import these pyrimidines into plastids is PLUTO (Figure 9).

This hypothesis explains the high importance of pyrimidine salvage activity in plastids. Plastidic isoforms of both UPRT and uridine kinase represent by far the highest activities in *Arabidopsis* tissues (Mainguet et al., 2009; Chen and Thelen, 2011). The corresponding genes, *UPP*, *UKL1*, and *UKL2*, have been characterized in detail at the biochemical level. Furthermore, mutants lacking the activity of UPRT or uridine kinase are characterized by severe growth defects and chlorosis (Mainguet et al., 2009; Chen and Thelen, 2011). Thus, plastidic pyrimidine salvage is well understood and ultimately required for proper plant development. In tobacco (*Nicotiana tabacum*) Bright Yellow 2 cells, downregulation of pyrimidine salvage and de novo synthesis were identified as early signals in programmed cell death (Stasolla et al., 2004). It will be an exciting task for the future to evaluate the role of PLUTO in balancing pyrimidine salvage activity and de novo synthesis.

Further substrates of PLUTO are the purine nucleobases guanine and adenine. Therefore, participation in pyrimidine salvage is apparently not the only function of PLUTO. However, metabolism of purine nucleobases in plastids is not well understood. To our knowledge, the only enzyme accepting adenine as substrate is adenine phosphoribosyltransferase (APRT). APRTs form a small gene family in *Arabidopsis* comprising five members. According to prediction software, APRT1 exhibits plastidic targeting (Schwacke et al., 2003). However, in an analysis of APRT1-3, it was suggested that the respective proteins are cytosolic (Allen et al., 2002). The apparent high affinities of APRT1-3 in the range of 0.8 to 2.6 μM (Allen et al., 2002) are comparable to that of PLUTO, indicating that adenine concentrations in plants are low. Nevertheless, this aspect requires further experimental efforts to link import of adenine into plastids to purine salvage. The same holds true for metabolism of guanine.

At the same time, such compartmentation of pyrimidine de novo synthesis implies that carbamoyl aspartate has to be exported from the plastid. So far no transport protein is known to accept this metabolite as substrate. However, carbamoyl aspartate represents a modified amino acid and may be accepted as transport substrate by amino acid permeases, many of which have been identified. In plastids, members of the DIT protein family have been shown to transport a range of amino acids and dicarboxylic acids, as well as Asp (Renné et al., 2003). Furthermore, two members of the amino acid/auxin permease family (Weber et al., 2005) are predicted to be plastidic. These proteins might be candidates for such a required transport function.

METHODS

Strains and Media

For heterologous expression studies and uptake experiments, an *Escherichia coli* transposon insertion strain lacking the endogenous uracil

permease uraA (JD23420) was ordered from the National Institute of Genetics (Shizuoka, Japan; http://www.shigen.nig.ac.jp/ecoli/strain/top/top.jsp) and grown in YT medium (0.8% peptone, 0.5% yeast extract, and 0.25% NaCl) with or without ampicillin (50 mg L^{-1}) and kanamycin (25 mg L^{-1}). Plasmids were propagated in *E. coli* cells (XL1Blue; Stratagene) and grown in YT medium with or without ampicillin (50 mg L^{-1}) and tetracycline (2.5 mg L^{-1}).

Isolation of Cauliflower Bud Amyloplasts

Cauliflower (*Brassica oleracea* cv botrytis) floral buds were purchased from the local market. Cauliflower bud amyloplasts used for uracil uptake studies were isolated according to the method of Journet and Douce (1985), modified as described by Neuhaus et al. (1993). The isolated plastids were resuspended in a medium consisting of 15 mM HEPES-KOH, pH 7.2, 2 mM $MgCl_2$, 1 mM EDTA, and 0.3 M sorbitol. The total protein concentration was determined according to the method of Bradford (1976).

Uptake Experiments with Isolated Cauliflower Bud Amyloplasts

The uracil uptake into isolated cauliflower bud amyloplasts was studied using the silicone-oil filtration method (Heldt and Sauer, 1971) with modifications (Batz et al., 1992). This method enables the quantitative separation of isolated plastids from the incubation medium by centrifugation. To study uracil uptake, 100 μL of the isolated cauliflower bud amyloplasts (2 mg protein/mL) was added to the same volume of an uptake medium consisting of 15 mM HEPES-KOH, pH 7.2, 2 mM $MgCl_2$, 1 mM EDTA, and 0.3 M sorbitol and [^{14}C]-uracil (10^{12} Bq mol^{-1}). Termination of the transport process was achieved by separation of the plastids from the incubation medium by centrifugation of the samples at 12,000*g* through the silicone oil (Microfuge E; Beckman; see details in Batz et al., 1992). Radioactivity appearing in the supernatant was quantified by beta counting in a Packard Tricarb 2500 (Packard). The values were corrected for transport substrate trapped within the sorbitol-permeable space of the plastids.

UPRT Enzyme Assay

UPRT activity was determined using a standard assay mixture consisting of 50 mM HEPES-KOH, pH 7.2, 5 mM $MgCl_2$, 10 mM NaN_3, 0,5 mM phosphoribosyl-pyrophosphate, 0.025% BSA, and 0.5 mM [^{14}C]-uracil (5×10^9 Bq mol^{-1}), which was assayed at 30°C and 300 rpm. The reaction was initiated by the addition of 10 μL cauliflower bud amyloplast suspension (5 to 10 mg · mL^{-1} protein) to the assay mixture and terminated by the addition of 1 mL ice-cold 50 mM sodium acetate, pH 5.0, and 2 mM KH_2PO_4. Nucleotides were precipitated with 100 mM $LaCl_3$, pH 5.0, and incubated for 30 min on ice. The mixture was then filtered through a membrane filter (0.45-μm pore size; Whatman). Then, the filter was transferred into a 5-mL scintillation vessel and filled with 4 mL scintillation cocktail (Roth). The radiolabeled generated UMP was measured by liquid scintillation counting in a Packard Tricarb 2500.

Generation and Transient Expression of GFP Fusion Constructs

For the construction of GFP fusion proteins, the entire cDNAs were amplified (with insertion of *Xba*I and *Xho*I cleavage sites and deletion of the native stop codon) by PCR using Pfu-DNA polymerase (Stratagene) with primers listed in Supplemental Table 1 online. The obtained PCR products were subcloned into an *Eco*RV-linearized pBluescript vector (Stratagene), cleaved using *Xba*I and *Xho*I, respectively, and fused translationally with the GFP coding region of the vector pGFP2 (Kost et al., 1998), leading to the final GFP constructs under the control of a 35S promoter. To analyze an N-terminal truncated PLUTO-GFP fusion protein with a missing target peptide, the PLUTO cDNA was amplified by PCR using Pfu-DNA polymerase (Stratagene) with primers PLUTO_short_pGFP2_fwd and PLUTO_pGFP2_rev (see Supplemental Table 1 online) and cloned as described above. Protoplasts isolated from *Arabidopsis thaliana* were transformed with column-purified plasmid DNA (Yoo et al., 2007). After 24 h of incubation at 22°C in the dark, protoplasts were analyzed and checked for the presence of green fluorescence with a Leica TCS SP5II microscope (488-nm excitation and 505- to 540-nm detection of emission through a ×63 1.2 water immersion objective). Chlorophyll autofluorescence was detected with 488-nm excitation and a 649- to 770-nm emission wavelength. For colocalization studies of DHODH with mitochondria, the mitotracker dye Orange CMTMRos 7510 (Invitrogen) was used. Protoplasts were incubated for 10 min with mitotracker (2 μM), and unincorporated dye was subsequently washed off. Mitotracker fluorescence was detected at 488-nm excitation with 580- to 620-nm emission wavelength. Transient expression studies of *PLUTO* in onion (*Allium cepa*) epidermal peels were achieved by biolistic transformation (Sambrook and Russell, 2001). Labeling of cell wall, plasma membrane, and internal membranes by the fluorescent dye FM4-64 (T13320; Invitrogen) was achieved by incubating onion epidermal peels for 10 min in FM4-64 (2 μM) and washing off unincorporated dye. FM4-64 fluorescence was detected at 488 nm excitation with 613- to 704-nm emission wavelength. The obtained data were analyzed with Leica confocal software.

Heterologous Expression of PLUTO in *E. coli* JD23420

For heterologous expression of *PLUTO* in *E. coli*, *PLUTO* was amplified with Pfu-DNA polymerase using the construct pBSK:*PLUTO* as a template and the primers PLUTO_pTACMAT2_fwd with an *Xho*I restriction site and PLUTO_pTACMAT2_rev with a *Kpn*I restriction site (see Supplemental Table 1 online). For the generation of the N-terminal truncated *PLUTO* expression construct, primer PLUTO_pTACMAT2k_fwd was used (see Supplemental Table 1 online). The obtained PCR products for *PLUTO* were cleaved and cloned into the *Xho*I-*Kpn*I restriction site of the bacterial expression vector pTAC-MAT-Tag-2 (Sigma-Aldrich). For uptake experiments, these constructs were transformed in *E. coli* cells (JD23420; National Institute of Genetics, Shizuoka, Japan). Cells transformed with the *PLUTO* expression plasmids were inoculated with an overnight culture and grown at 37°C in YT medium containing ampicillin and kanamycin. An OD_{600} value of 0.5 was required for the initiation of *PLUTO* expression by addition of isopropyl β-D-1-thiogalactopyranosid (final concentration of 0.02%). Cells were grown for 1.5 h after induction, and 50 mL was collected by centrifugation for 5 min at 4500*g* at 4°C. The sediments were resuspended to an OD_{600} value of 5 using potassium phosphate buffer (50 mM, pH 7.0) and stored on ice until use.

Uptake of Radioactively Labeled Nucleobases in *E. coli*

IPTG-induced *E. coli* cells and noninduced control cells (100 μL) harboring the PLUTO expression plasmids were added to the same volume of potassium phosphate buffer (50 mM, pH 7.0) containing [^{14}C]-uracil, -guanine, or -adenine (10^{12} Bq mol^{-1}). To test the effect of NaCl, LiCl (as a control), and the uncoupler carbonylcyanide CCCP, these substances were previously added in the indicated concentrations to the incubation medium of the bacterial cells. The uptake of nucleobases (20 μM, if not indicated otherwise) was performed at 37°C and 200 rpm in a reaction vessel incubator and terminated by vacuum filtration of the cells through a membrane filter (0.45-μm pore size; Whatman) moistened with potassium phosphate buffer (50 mM, pH 7.0). Cells were washed to remove unimported nucleobases (three times with 1 mL potassium phosphate buffer, 50 mM, pH 7.0). The filter was transferred into a 5-mL scintillation

vessel and filled with 4 mL of scintillation cocktail (Roth). Radioactivity in the samples was quantified in a Packard Tricarb 2500 scintillation counter (Packard). To check for periplasmic cleavage of uridine after incubation with *PLUTO*-expressing *E. coli* cells, supernatants and pelleted bacterial cells were subjected to thin layer chromatography as described by Jung et al. (2009).

Quantitative RT-PCR

Quantitative RT-PCR was performed as described (Leroch et al., 2005). Total RNA was prepared from *Arabidopsis* plants using the RNeasy plant mini kit (Qiagen). To remove any contaminating DNA, the samples were treated with DNase (RNase-free DNase kit; Qiagen). Quantitative PCR was performed using a MyIQ-Cycler (Bio-Rad) and IQ SYBR Green Supermix (Bio-Rad) according to the manufacturer's instructions with the following cycler conditions: 3 min at 95°C, 40 cycles of 15 s at 95°C, 25 s at 58°C, and 40 s at 72°C followed by 1 min at 95°C. Gene-specific primers used are listed in Supplemental Table 1 online. The gene *EF1α* (At1g07930), encoding elongation factor 1α, was used for quantitative normalization (Curie et al., 1991).

Construction of the Sequence Alignment

Multiple alignments of protein sequences were performed with the program ClustalW (Thompson et al., 1994).

Accession Numbers

Sequence data from this article can be found in the Arabidopsis Genome Initiative or GenBank/EMBL databases under the following accession numbers: PLUTO (At5g03555; AED90625); FUR4 (P05316), uracil transporter of *Saccharomyces cerevisiae*; FUI1 (P38196), uridine transporter of *S. cerevisiae*; HYUP (Q9F467), a transport protein of *Arthrobacter aurescens*; PUCI (P94575), allantoin transporter of *Bacillus subtilis*; DAL4 (Q04895), allantoin transporter of *S. cerevisiae*; and MHP1 (2JLN_A), transport protein of *Microbacterium liquefaciens*.

Supplemental Data

The following materials are available in the online version of this article.

Supplemental Figure 1. Thin Layer Chromatography of Reaction Products after Incubation of Uridine with *PLUTO*-Expressing *E. coli* Cells.

Supplemental Figure 2. Transient Expression of *PLUTO-GFP* in *Allium cepa* (Onion) Epidermal Cells.

Supplemental Table 1. Primers Used in This Study.

ACKNOWLEDGMENTS

This work was supported by Deutsche Forschungsgemeinshaft Grant MO 1032/3-1. We thank Ekkehard Neuhaus for supporting this work.

AUTHOR CONTRIBUTIONS

S.W. performed research on PLUTO. B.J. designed and performed research on pyrimidine de novo synthesis. S.F. assisted in cloning work and protoplast preparation. T.M. designed research and wrote the article.

Received February 17, 2012; revised March 14, 2012; accepted March 22, 2012; published April 3, 2012.

REFERENCES

Allen, M., Qin, W., Moreau, F., and Moffatt, B. (2002). Adenine phosphoribosyltransferase isoforms of Arabidopsis and their potential contributions to adenine and cytokinin metabolism. Physiol. Plant. **115:** 56–68.

Batz, O., Scheibe, R., and Neuhaus, H.E. (1992). Transport processes and corresponding changes in metabolite levels in relation to starch synthesis in barley (*Hordeum vulgare L.*) etioplasts. Plant Physiol. **100:** 184–190.

Bradford, M.M. (1976). A rapid and sensitive method for the quantitation of microgram quantities of protein utilizing the principle of protein-dye binding. Anal. Biochem. **72:** 248–254.

Brady, B.S., Hyman, B.C., and Lovatt, C.J. (2010). Regulation of CPSase, ACTase, and OCTase genes in *Medicago truncatula*: Implications for carbamoylphosphate synthesis and allocation to pyrimidine and arginine de novo biosynthesis. Gene **462:** 18–25.

Chen, C.T., and Slocum, R.D. (2008). Expression and functional analysis of aspartate transcarbamoylase and role of *de novo* pyrimidine synthesis in regulation of growth and development in Arabidopsis. Plant Physiol. Biochem. **46:** 150–159.

Chen, M., and Thelen, J.J. (2011). Plastid uridine salvage activity is required for photoassimilate allocation and partitioning in *Arabidopsis*. Plant Cell **23:** 2991–3006.

Chevallier, M.R., and Lacroute, F. (1982). Expression of the cloned uracil permease gene of *Saccharomyces cerevisiae* in a heterologous membrane. EMBO J. **1:** 375–377.

Cornelius, S., Witz, S., Rolletschek, H., and Möhlmann, T. (2011). Pyrimidine degradation influences germination seedling growth and production of Arabidopsis seeds. J. Exp. Bot. **62:** 5623–5632.

Curie, C., Liboz, T., Bardet, C., Gander, E., Médale, C., Axelos, M., and Lescure, B. (1991). Cis and trans-acting elements involved in the activation of *Arabidopsis thaliana* A1 gene encoding the translation elongation factor EF-1 alpha. Nucleic Acids Res. **19:** 1305–1310.

Emanuelsson, O., Nielsen, H., and von Heijne, G. (1999). ChloroP, a neural network-based method for predicting chloroplast transit peptides and their cleavage sites. Protein Sci. **8:** 978–984.

Furumoto, T., et al. (2011). A plastidial sodium-dependent pyruvate transporter. Nature **476:** 472–475.

Geigenberger, P., Riewe, D., and Fernie, A.R. (2010). The central regulation of plant physiology by adenylates. Trends Plant Sci. **15:** 98–105.

Heldt, H.W., and Sauer, F. (1971). The inner membrane of the chloroplast envelope as the site of specific metabolite transport. Biochim. Biophys. Acta **234:** 83–91.

Journet, E.-P., and Douce, R. (1985). Enzymic capacities of purified cauliflower bud plastids for lipid synthesis and carbohydrate metabolism. Plant Physiol. **79:** 458–467.

Joyce, G.F. (2002). The antiquity of RNA-based evolution. Nature **418:** 214–221.

Jund, R., Weber, E., and Chevallier, M.R. (1988). Primary structure of the uracil transport protein of *Saccharomyces cerevisiae*. Eur. J. Biochem. **171:** 417–424.

Jung, B., Flörchinger, M., Kunz, H.H., Traub, M., Wartenberg, R., Jeblick, W., Neuhaus, H.E., and Möhlmann, T. (2009). Uridine-ribohydrolase is a key regulator in the uridine degradation pathway of *Arabidopsis*. Plant Cell **21:** 876–891.

Jung, B., Hoffmann, C., and Möhlmann, T. (2011). Arabidopsis nucleoside hydrolases involved in intracellular and extracellular degradation of purines. Plant J. **65:** 703–711.

Kafer, C., Zhou, L., Santoso, D., Guirgis, A., Weers, B., Park, S., and Thornburg, R. (2004). Regulation of pyrimidine metabolism in plants. Front. Biosci. **9:** 1611–1625.

Kirchberger, S., Tjaden, J., and Neuhaus, H.E. (2008). Characteriza-

tion of the Arabidopsis Brittle1 transport protein and impact of reduced activity on plant metabolism. Plant J. **56:** 51–63.

Kost, B., Spielhofer, P., and Chua, N.-H. (1998). A GFP-mouse talin fusion protein labels plant actin filaments in vivo and visualizes the actin cytoskeleton in growing pollen tubes. Plant J. **16:** 393–401.

Lehninger, A.L., Nelson, D.L., and Cox, M.M. (1994). Prinzipien der Biochemie, H. Tschesche, ed (Heidelberg, Berlin, Oxford: Spektrum Akademischer Verlag).

Leroch, M., Kirchberger, S., Haferkamp, I., Wahl, M., Neuhaus, H.E., and Tjaden, J. (2005). Identification and characterization of a novel plastidic adenine nucleotide uniporter from *Solanum tuberosum*. J. Biol. Chem. **280:** 17992–18000.

Mainguet, S.E., Gakière, B., Majira, A., Pelletier, S., Bringel, F., Guérard, F., Caboche, M., Berthomé, R., and Renou, J.P. (2009). Uracil salvage is necessary for early Arabidopsis development. Plant J. **60:** 280–291.

Mitterbauer, R., Karl, T., and Adam, G. (2002). *Saccharomyces cerevisiae* URH1 (encoding uridine-cytidine N-ribohydrolase): Functional complementation by a nucleoside hydrolase from a protozoan parasite and by a mammalian uridine phosphorylase. Appl. Environ. Microbiol. **68:** 1336–1343.

Möhlmann, T., Bernard, C., Hach, S., and Neuhaus, H.E. (2010). Nucleoside transport and associated metabolism. Plant Biol. (Stuttg.) **12** (suppl. 1)**:** 26–34.

Möhlmann, T., Scheibe, R., and Neuhaus, H.E. (1994). Interaction between starch synthesis and fatty-acid synthesis in isolated cauliflower-bud amyloplasts. Planta **194:** 492–497.

Neuhaus, H.E., Henrichs, G., and Scheibe, R. (1993). Characterization of glucose-6-phosphate incorporation into starch by isolated intact cauliflower-bud plastids. Plant Physiol. **101:** 573–578.

Neuhaus, H.E., Thom, E., Möhlmann, T., Steup, M., and Kampfenkel, K. (1997). Characterization of a novel eukaryotic ATP/ADP translocator located in the plastid envelope of *Arabidopsis thaliana* L. Plant J. **11:** 73–82.

Renné, P., Dressen, U., Hebbeker, U., Hille, D., Flügge, U.I., Westhoff, P., and Weber, A.P. (2003). The Arabidopsis mutant dct is deficient in the plastidic glutamate/malate translocator DiT2. Plant J. **35:** 316–331.

Riegler, H., Geserick, C., and Zrenner, R. (2011). *Arabidopsis thaliana* nucleosidase mutants provide new insights into nucleoside degradation. New Phytol. **191:** 349–359.

Sambrook, J., and Russell, D.W. (2001). Molecular Cloning: A Laboratory Manual, 3rd ed. (Cold Spring Harbor, NY: Cold Spring Harbor Laboratory Press).

Saier, M.H., Jr., Yen, M.R., Noto, K., Tamang, D.G., and Elkan, C. (2009). The Transporter Classification Database: Recent advances. Nucleic Acids Res. **37**(Database issue): D274–D278.

Schröder, M., Giermann, N., and Zrenner, R. (2005). Functional analysis of the pyrimidine *de novo* synthesis pathway in solanaceous species. Plant Physiol. **138:** 1926–1938.

Schwacke, R., Schneider, A., van der Graaff, E., Fischer, K., Catoni, E., Desimone, M., Frommer, W.B., Flügge, U.I., and Kunze, R. (2003). ARAMEMNON, a novel database for Arabidopsis integral membrane proteins. Plant Physiol. **131:** 16–26.

Shibata, H., Ochiai, H., Sawa, Y., and Miyoshi, S. (1986). Localization of carbamoylphosphate synthetase and aspartate carbamoyltransferase in chloroplasts. Plant Physiol. **80:** 126–129.

Slocum, R.D. (2005). Genes, enzymes and regulation of arginine biosynthesis in plants. Plant Physiol. Biochem. **43:** 729–745.

Stasolla, C., Loukanina, N., Yeung, E.C., and Thorpe, T.A. (2004). Alterations in pyrimidine nucleotide metabolism as an early signal during the execution of programmed cell death in tobacco BY-2 cells. J. Exp. Bot. **55:** 2513–2522.

Thompson, J.D., Higgins, D.G., and Gibson, T.J. (1994). CLUSTAL W: Improving the sensitivity of progressive multiple sequence alignment through sequence weighting, position-specific gap penalties and weight matrix choice. Nucleic Acids Res. **22:** 4673–4680.

Ullrich, A., Knecht, W., Piskur, J., and Löffler, M. (2002). Plant dihydroorotate dehydrogenase differs significantly in substrate specificity and inhibition from the animal enzymes. FEBS Lett. **529:** 346–350.

Watanabe, K., Tomioka, S., Tanimura, K., Oku, H., and Isoi, K. (2011). Uptake of AMP, ADP, and ATP in *Escherichia coli* W. Biosci. Biotechnol. Biochem. **75:** 7–12.

Weber, A.P., Schwacke, R., and Flügge, U.I. (2005). Solute transporters of the plastid envelope membrane. Annu. Rev. Plant Biol. **56:** 133–164.

Werner, A.K., and Witte, C.P. (2011). The biochemistry of nitrogen mobilization: Purine ring catabolism. Trends Plant Sci. **16:** 381–387.

Weyand, S., et al. (2008). Structure and molecular mechanism of a nucleobase-cation-symport-1 family transporter. Science **322:** 709–713.

Yoo, S.-D., Cho, Y.-H., and Sheen, J. (2007). Arabidopsis mesophyll protoplasts: A versatile cell system for transient gene expression analysis. Nat. Protoc. **2:** 1565–1572.

Zimmermann, P., Hirsch-Hoffmann, M., Hennig, L., and Gruissem, W. (2004). GENEVESTIGATOR. Arabidopsis microarray database and analysis toolbox. Plant Physiol. **136:** 2621–2632.

Zrenner, R., Riegler, H., Marquard, C.R., Lange, P.R., Geserick, C., Bartosz, C.E., Chen, C.T., and Slocum, R.D. (2009). A functional analysis of the pyrimidine catabolic pathway in Arabidopsis. New Phytol. **183:** 117–132.

Zrenner, R., Stitt, M., Sonnewald, U., and Boldt, R. (2006). Pyrimidine and purine biosynthesis and degradation in plants. Annu. Rev. Plant Biol. **57:** 805–836.